# GaInAsP/InP Quantum-Wire Lasers Fabricated by Low-Damage Dry-Etching Process

*Shigehisa ARAI, Nobuhiro NUNOYA, Madoka NAKAMURA, Hideo YASUMOTO, Qiguang YANG, Monir MORSHED, Hideki MIDORIKAWA, and Mothi Madhan RAJ
Research Center for Quantum Effect Electronics, Tokyo Institute of Technology
2-12-1 O-okayama, Meguro-ku, Tokyo 152-8552, Japan
Phone: +81-3-5734-2512, Fax: +81-3-5734-2907, E-mail: arai@pe.titech.ac.jp

## Abstract

The advancement in the research of GaInAsP/InP 1.5μm wavelength quantum-wire lasers by 2-step organo-metallic vapor-phase-epitaxy and electron-beam-lithography is presented. By using a wet-chemical etching, higher performance as well as narrower material gain spectrum of single-layer quantum-wire lasers over quantum-film lasers was obtained at a temperature below 200K. In order to realize high density multiple-layered quantum-wire structure, a low-damage $CH_4/H_2$ reactive-ion-etching followed by a wet-cleaning process was developed and was characterized by PL intensity dependence on the wire width. Using this fabrication process, very low threshold current density operation (330A/cm$^2$: @RT) of 5-quantum-well distributed feedback lasers as well as double-layered quantum-wire laser with the threshold current density lower than the single-layer quantum-wire laser fabricated by the wet-chemical etching was obtained.

## 1. Introduction

Aiming at high performance semiconductor lasers with low threshold current, high efficiency and narrow linewidth properties, low-dimensional structures have been investigated extensively[1]-[3]. We have reported the fabrication and characterizations of GaInAsP/InP long wavelength quantum-wire (Q-Wire) lasers made by electron-beam-lithography (EBL) and a wet-chemical etching followed by organo-metallic vapor-phase-epitaxy (OMVPE)[4],[5]. This method is considered to be superior to other methods in order to utilize an advantage of bi-axially strained quantum-well (QW) structures, i.e. stronger lateral quantum-confinement effect due to reduced effective mass of holes in either one of heavy-hole and light-hole bands[6], [7].

Room temperature (RT) continuous wave (CW) operations were obtained for 3-layered lattice-matched (LM) Q-Wire (10-30nm width) lasers[8], 3-layered compressively-strained (CS) Q-Wire (30-60nm) lasers[9], and single-layer tensile-strained (TS) Q-Wire (30-40nm) lasers[10], but superior lasing properties over quantum-film (Q-Film) lasers were not obtained even in low temperature region because of too large variation of wire width of the stacked multiple wires or too wide wire structures. Then we realized Q-Wire lasers with narrower wire width fabricated from 1% CS single Q-Film structure, and obtained lower threshold current as well as higher differential quantum efficiency than Q-Film lasers at temperature below 200K[11]. Polarization dependent photoluminescence (PL) property was also confirmed and its anisotropy was found to be stronger in the CS-Q-Wire structure than in LM-Q-Wire structure[12]. From gain spectrum measurements, the material gain in the CS-Q-Wire structure was found to be slightly narrower than that in the initial Q-Film structure[13].

In this paper, we would like to present recent results on GaInAsP/InP CS-Q-Wire lasers. In section 2, some lasing properties of single-layer CS-Q-Wire lasers fabricated by wet-chemical etching followed by OMVPE regrowth are presented. In section 3, fine structure fabrication by $CH_4/H_2$ reactive-ion-etching (RIE) followed by a wet-cleaning and the damage characterization are given. In section 4, applications of the above mentioned process, i.e. distributed-feedback (DFB) lasers with completely etched active region and double-layered CS-Q-Wire lasers, are presented.

## 2. CS-Q-Wire lasers by wet-chemical etching

Our fabrication method consists of 4 steps, i.e. (a) growth of an initial wafer containing an active layer, (b) formation of a fine pattern using EB direct writing, (c) pattern transfer to the wafer by (wet or dry) etching, and (d) regrowth on the patterned wafer by OMVPE. Figure 1 shows cross sectional SEM views of two CS-Q-Wire lasers fabricated by wet etching technique, where quantum-wires were made perpendicular to the stripe direction (<011>, stripe width: 15μm) so as to take an advantage of larger dipole moment for TE modes. The width of the quantum-wire of the left one is 25nm (Q-Wire25 for short, period Λ=70nm) and that of the right one is 20nm (Q-Wire20, Λ=50nm).

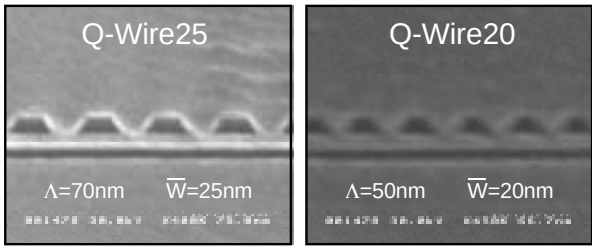


Fig. 1 Cross sectional SEM views of Q-Wire lasers

We measured I-L characteristics of these Q-Wire lasers at various temperatures and compared with those of Q-Film lasers prepared on the same wafer.. As the result, threshold current density ($J_{th}$) of the Q-Wire lasers reduced drastically with reducing the temperature and became almost half that of the Q-Film lasers at around $T$=100K, whereas it was about 4 times higher at RT. From the cavity length dependences of threshold current ($I_{th}$), $J_{th}$ and differential quantum efficiency ($\eta_d$) at $T$=90K as listed in Table 1, the internal quantum efficiency ($\eta_i$) was evaluated to be almost 1. Poor lasing properties of the Q-Wire lasers at around RT might be attributed to gain saturation at high injection level due to very small optical confinement factor $\xi$ of the active region and rapid non-radiative recombination process at regrown interfaces. A realization of uniform and high density Q-Wire structure is required for high performance operation of Q-Wire lasers.

Table 1 Lasing properties of Q-Wire20 at 90 K

| L [μm] | $I_{th}$ [mA] | $J_{th}$ [A/cm$^2$] | $\eta_d$ [%] |
|---|---|---|---|
| 1020 | 6.0 | 38 | 61 |
| 670 | 4.0 | 39 | 69 |
| 400 | 6.5 | 105 | 86 |

## 3. $CH_4/H_2$ RIE for Q-Wire structure

First we investigated fundamental properties of $CH_4/H_2$ RIE of GaInAsP/InP heterostructures, e.g. etch rate, mesa shape under a certain mask and damage induced by RIE. In our $CH_4/H_2$ RIE, the etch rate was about 10nm/min for the groove width of 30-40nm under conditions of gas flow rate of $CH_4$:$H_2$. =10:40 (sccm), pressure of 6.5Pa and RF power of 100W. In order to remove polymer deposited during the etching, $O_2$ ashing was done after an interval of 5-10min. etching, and this etching/ashing sequence was repeated several times. Then slight amount of wet-chemical etching (cleaning) was done to remove damaged layer and the sample was underwent OMVPE regrowth.

After the dry etching, the sample was embedded in undoped InP by OMVPE at 600℃ with relatively slow growth rate (250nm/h: 1/5 of conventional one). Figure 2 shows schemata and SEM photographs of a CS-5MQW structure with 100nm period after dry etching (upper) and embedding growth (lower). As can be seen, a good vertical shaped mesa structure was obtained after the RIE, but one or two QWs were missing after the regrowth. This might happen during the wet cleaning process because of poor adhesion of $SiO_2$ mask to the top InP layer of the wafer.

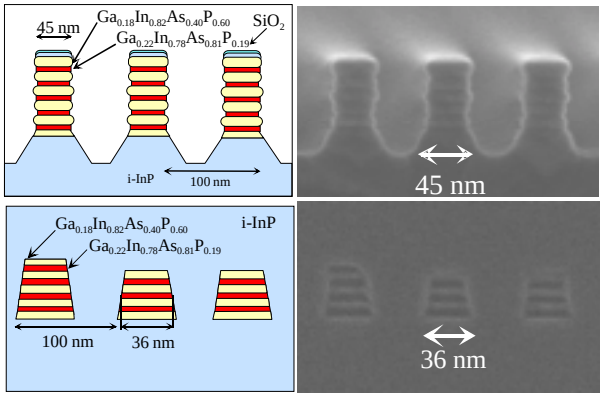


Fig. 2 Schemata and SEM views of multiple-layered wire structures.

In order to evaluate the quality of the etched surface as well as regrown interfaces, PL intensity was measured at RT for wire structures with various widths ($W$). The PL intensity of a wire structure $I_{wire}$ normalized by the space filling factor ρ (=$W/\Lambda$) can be given by the following relation,

$$\frac{I_{wire}/\rho}{I_{film}} = \frac{1}{1+\dfrac{2\cdot S\cdot\tau}{W-2W_d}}$$

where $S$ is the surface recombination velocity, τ is carrier lifetime, $W_d$ is dead-layer thickness[14]. Figure 3 shows measured normalized PL intensities as a function of the wire width and fitting curves obtained by the relation above (where $W_d$ =0 was assumed). As can be seen, surface recombination rate, which can be evaluated by the product $S\tau$, of mesa etched sample was not improved by the wet cleaning ($S\tau$=750nm, indicated by open circles and triangles), but it was drastically improved after the embedding growth ($S\tau$=28nm, indicated by painted squares). This result indicates the $CH_4/H_2$-RIE and OMVPE regrowth process can be used for lasers consisting of wire-like active region as narrow as 100nm.

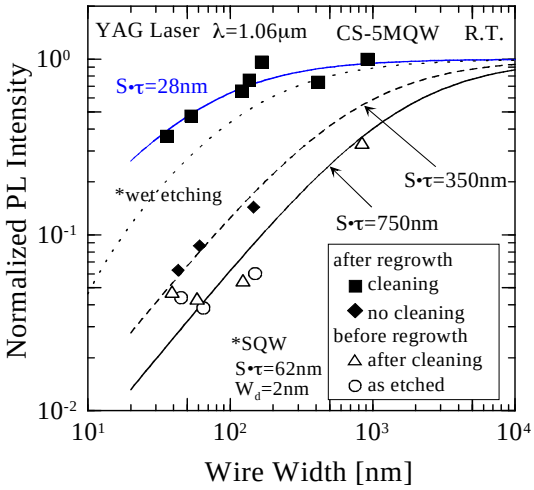


Fig. 3 Normalized PL intensity

## 4. Multiple-layered DFB and Q-Wire lasers

Using above mentioned fabrication process, we tried to realize DFB and Q-Wire lasers by using various periods of wire patterns on a same wafer.

### 4.1 Low threshold DFB lasers

Figure 4 shows an SEM photograph (on the left) and schema of CS-5MQW-DFB laser with the grating period of Λ =240nm. Even though a slight undercut etching is observed, quite smooth regrown surfaces of i-InP and i-GaInAsP optical confinement layers (OCL) were obtained. The active region width

is 175nm and an index-coupling coefficient of the grating is estimated to be $\kappa_i$ =290cm$^{-1}$, hence this structure can be applied to short cavity DFB lasers for extremely low threshold current operation.

Figure 5 shows I-L characteristics of four different types of mesa etched stripe lasers (stripe width $W_s$ = 20μm) as well as their parameters (in the lower table). Threshold current density $J_{th}$ as low as 330A/cm$^2$ was obtained for DFB lasers, which was about a half that of the Q-Film laser[15]. On the other hand in the non-DFB laser (Λ =200nm), slightly higher differential quantum efficiency $\eta_d$ was obtained while $J_{th}$ was almost same as that of the Q-Film laser.

Recently an extremely low threshold current density $J_{th}$ =94A/cm$^2$ ($I_{th}$=11mA @L=600μm, $W_s$ = 19.5μm) operation was obtained with a DFB laser with double-layered wire structure (width 83nm) active regions[16].

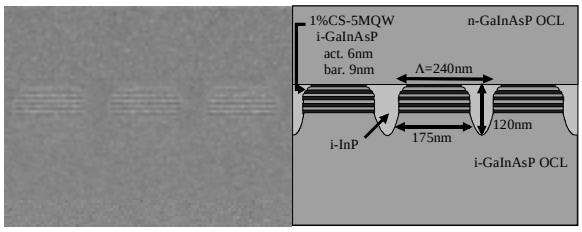


Fig.4 Cross sectional SEM view and illustration of DFB laser

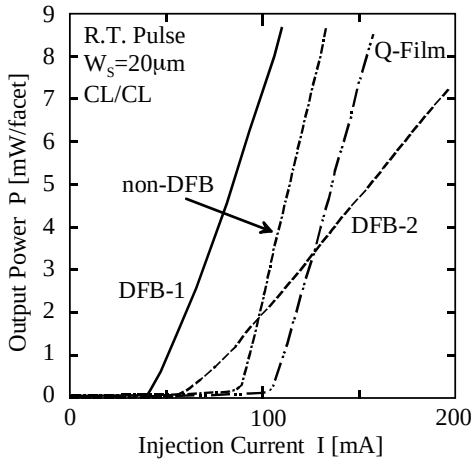


| | | L [μm] | $I_{th}$[mA] | $J_{th}$ [A/cm$^2$] | $\eta_d$ [%] | W [nm] | ξ [%] |
|---|---|---|---|---|---|---|---|
| Q-Film | | 760 | 103 | 680 | 38 | — | 5.08 |
| non-DFB | Λ=200nm | 620 | 83 | 670 | 46 | 126 | 3.20 |
| DFB-1 | Λ=240nm | 620 | 43 | 347 | 29 | 175 | 3.70 |
| DFB-2 | Λ=240nm | 860 | 57 | 330 | 12 | 175 | 3.70 |

Fig. 5 I-L characteristics of DFB lasers

### 4.2 Multiple-layered Q-Wire lasers

By the same process mentioned before, we could obtain multiple-layered Q-Wire lasers even though a few layers were missed during the wet-cleaning process before the OMVPE regrowth. Figure 6 shows schemata and SEM photographs of Q-Wire lasers with the wire width of (a) 52nm (Λ =120nm, Wire-like, $N_w$=3) and (b) 21nm. (Λ =120nm, Q-Wire, $N_w$=2). The width of etched groove was 70-80nm for the depth of 100nm.

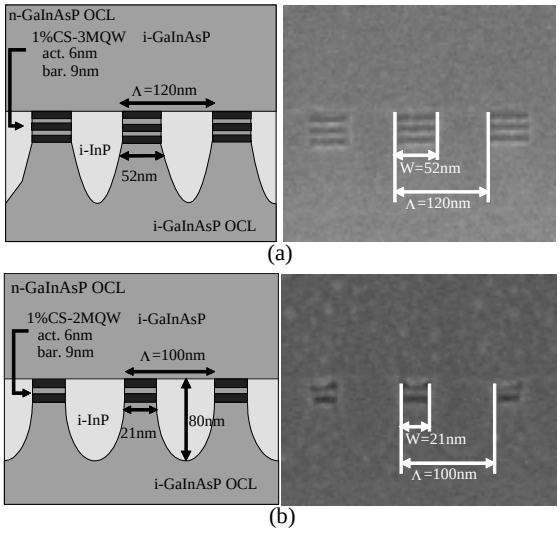


Fig. 6 Schemata and SEM views of Q-Wire lasers, (a) period 120 nm, wire width 52 nm, (b) period 100 nm, wire width 21 nm.

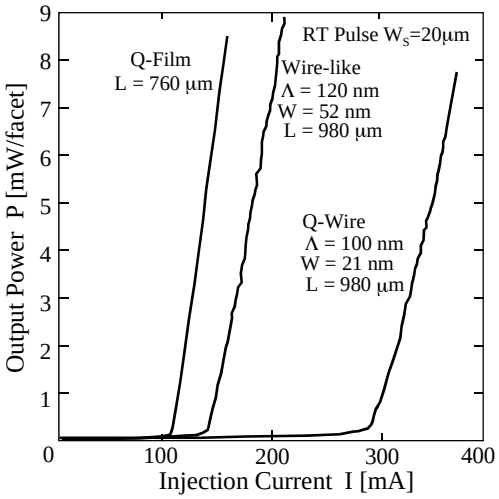


Fig. 7 I-L characteristics of wire lasers

Table 2 Lasing properties of Q-Wire and Q-Film lasers

| | L [μm] | $I_{th}$ [mA] | $J_{th}$ [A/cm$^2$] | $\eta_d$ [%] | $N_W$ | W [nm] | ξ [%] |
|---|---|---|---|---|---|---|---|
| Q-Film | 760 | 103 | 680 | 38 | 5 | | 5.08 |
| Wire-like (dry) Λ=120nm | 980 | 137 | 700 | 29 | 3 | 52 | 1.13 |
| Q-Wire2 (dry) Λ=100nm | 980 | 285 | 1450 | 20 | 2 | 21 | 0.32 |
| Q-Wire (Wet) Λ=70nm | 1050 | 390 | 2400 | 15 | 1 | 25 | 0.46 |

Figure 7 shows I-L characteristics of these lasers (20μm wide mesa etched stripe) and the Q-Film laser shown in Fig. 5. Among number of samples tested, lowest $J_{th}$ device for each group is shown here. Their lasing characteristics and structural parameters are summarized in Table 2, where those of the Q-Wire laser by wet-chemical etching are also listed for comparison[11]. $J_{th}$ of Q-Wire was 1.45kA/cm$^2$, which is still twice higher than that of the Q-Film laser but

is much lower than the Q-Wire laser by wet-chemical etching. This fact indicates that the $CH_4/H_2$-RIE/wet-cleaning process is almost comparable to wet-chemical etching at RT.

Temperature dependencies of (a) threshold current density $J_{th}$ and (b) lasing wavelength λ of these lasers were measured as shown in Fig. 8, where measured samples are not the same as those listed in Table 2 but are almost same quality ones. The characteristic temperatures $T_0$ of Q-Wire lasers were less than a half of that of the Q-Film laser at $T$>150K, and $J_{th}$ of the Q-Wire lasers was lower than that of the Q-Film laser at $T$<210-260K. At $T$=100K, $J_{th}$ =100A/cm$^2$ was obtained for the Q-Film laser and it was 40-45A/cm$^2$ for Q-Wire lasers. Taking into account the active region volume, $J_{th}$ of Q-Wire lasers is still 1.8 times (Wire-like laser) to 7 times (Q-Wire) higher than that of the Q-Film laser. Since this can be attributed to gain saturation in the Q-Wire structures due to very small optical confinement factor ξ, high density structure by reducing the period Λ is required to make better comparison.

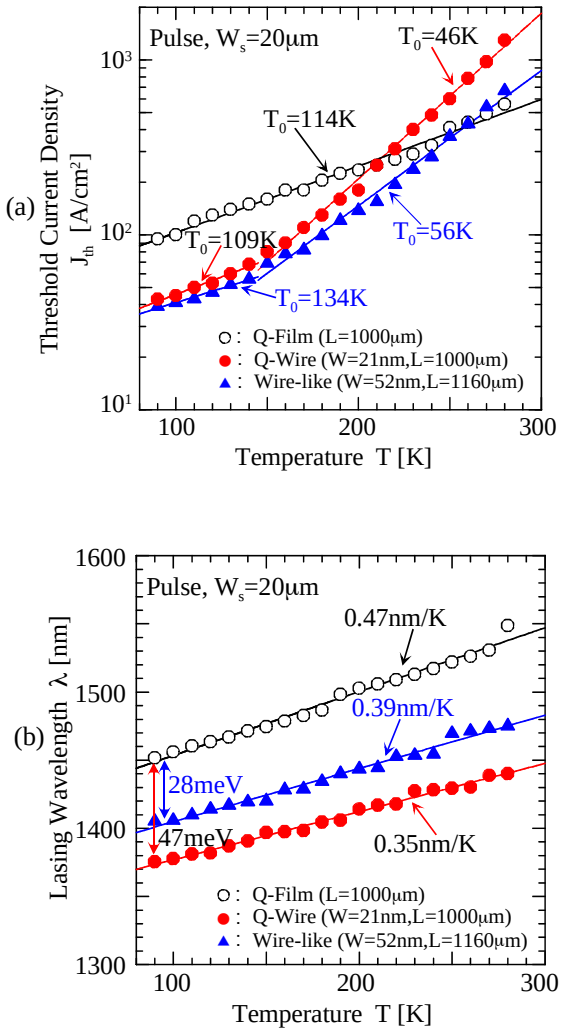


Fig. 8 Temperature dependences of
(a) threshold current density, and
(b) lasing wavelength.

As can be seen in Fig. 8(b), lasing wavelengths of Q-Wire lasers were quite shorter than that of the Q-Film laser. Similar shift was observed in EL peak wavelength at the bias current much lower than the threshold. These wavelength shifts correspond to energy blue shifts of 28meV (Wire-like laser) and 47meV (Q-Wire), which are much larger than those expected from the measured wire widths. The reason for this is considered to be higher carrier density in Q-Wire lasers and a reduction of an effective wire width due to 3-dimensional stress on the side-edge of quantum wires because compressively-strained active region is surrounded by InP and GaInAsP lattice-matched to InP.

The material gain spectra of these lasers (Q-Film and Wire-like) were obtained from the modal gain measurement by the Hakki-Paoli method under CW condition at $T$=100K. Figure 9(a) and 9(b) show the modal gain spectra and the material gain spectra, respectively, of these lasers at a bias current little below the threshold. As can be seen, the modal gain spectrum of the Wire-like laser was slightly wider than that of the Q-Film laser. However the material gain spectrum of the Q-Wire1 laser, which was obtained by normalizing the modal gain by the optical confinement factor ξ, was found to be narrower than that of the Q-Film laser.

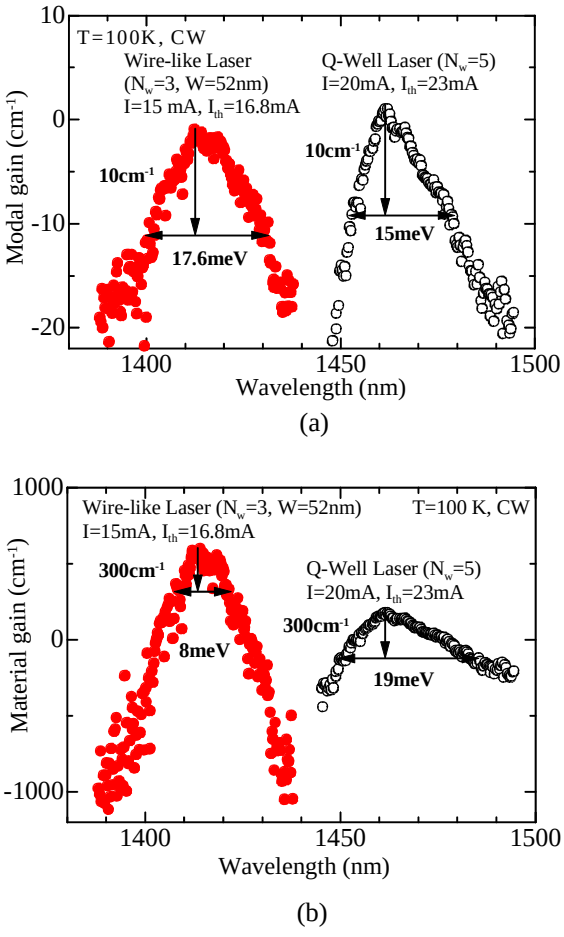


Fig. 9 (a) Modal gain spectra and (b) material gain spectra of Q-Film and Wire-like lasers.

In order to preserve all MQWs of the initial wafer after the dry-etching and the wet-cleaning process, we only increased the thickness of GaInAsP OCL on the top QW to 30nm. Figure 10 shows a schema and an SEM view of a Q-Wire laser with the wire width of 42nm ($\Lambda$ =120nm). As can be seen, 5 stacked wire active regions are completely preserved and a quite good size uniformity of the stacked multiple wire structure was obtained[17].

Figure 11 shows I-L characteristics under RT pulsed condition of thus fabricated Wire-like laser and a Q-Film laser both prepared on the same wafer. Threshold current density as low as 540A/cm$^2$ was obtained (@L=1380μm), which was almost the same as that of the Q-Film laser. Though there still remains a problem of a steep increase of the threshold current at around room temperature, lasing characteristic better than previously reported one fabricated by a wet-chemical etching and OMVPE regrowth was realized. For further improvement of the lasing properties, much narrower wire structure should be realized by reducing the period of the pattern.

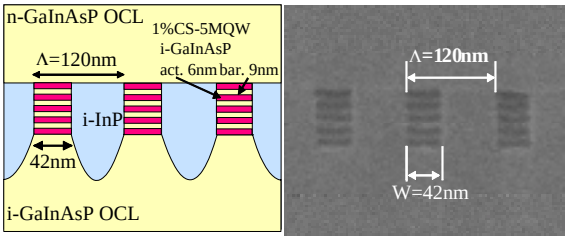


Fig. 10 Schema and an SEM view of a Wire-like laser with the wire width of 42nm.

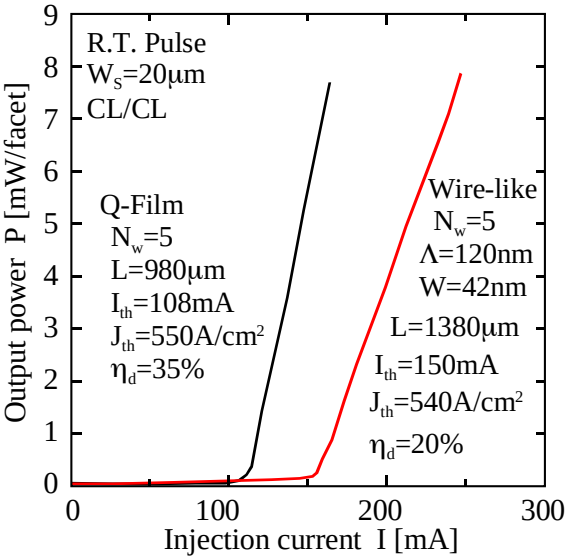


Fig. 11 I-L characteristics of a wire-like laser and a Q-Film laser prepared on the same wafer.

## 5. Conclusion

We realized room-temperature operation of multiple-layered GaInAsP/InP 1.5μm wavelength quantum-wire lasers by using $CH_4/H_2$ reactive-ion-etching and a wet-cleaning process followed by OMVPE embedding growth. Threshold current density as low as 1.45kA/cm$^2$ was obtained with double layered quantum-wire laser with the wire width of 21nm. The fabrication process employed here was very effective for low threshold current DFB lasers with strong index-coupling coefficient.


## Acknowledgment

The authors would like to thank Prof. Emeritus Y. Suematsu, Prof. K. Iga, Prof. K. Furuya, Prof. M. Asada, Assoc. Prof. F. Koyama, Assoc. Prof. Y. Miyamoto, Assoc. Prof. M. Watanabe and Dr. T. Miyamoto of Tokyo Institute of Technology for fruitful discussions. This research was financially supported by "Research for the Future Program (#JSPS-RFTF96P00101) of The Japan Society for the Promotion of Science and a Grant-In-Aid for a Scientific Research Project in a Priority Area "Single Electron Nano-electronics" and also for Fundamental Research B (#10450115) from the Ministry of Education, Science, Sports and Culture, Japan.


## References


[1] Y. Arakawa and H. Sakaki: Appl. Phys. Lett., **40** (1982) 939.

[2] M. Asada, Y. Miyamoto, and Y. Suematsu: IEEE J. Quantum Electron., **QE-22** (1986) 1915.

[3] Y. Miyake and M. Asada: Jpn. J. Appl. Phys., **28** (1989) 1280.

[4] Y. Miyamoto et al.: Jpn. J. Appl. Phys., **26** (1987)L225.

[5] P. Dasté et al.: J. Cryst. Growth: **93** (1988) 365.

[6] S. Ueno, Y. Miyake and M. Asada : Jpn. J. Appl. Phys., **31** (1992) 286.

[7] T. Yamauchi et al.: IEEE J. Quantum Electron., **QE-29** (1993) 2109.

[8] Y. Miyake et al. : IEEE J. Quantum Electron., **QE-29** (1993) 2123.

[9] K. Kudo et. al. : IEEE Photon. Technol. Lett., **4** (1992) 1089.

[10] K. Kudo et. al. : IEEE Photon. Technol. Lett., **5** (1993) 864.

[11] T. Kojima et al.: Jpn. J. Appl. Phys., **37** (1998) 4792.

[12] T. Kojima et al.: Jpn. J. Appl. Phys., **37** (1998) L46.

[13] T. Kojima et al.: Jpn. J. Appl. Phys., **37** (1998) L1386.

[14] M. Tamura et al.: Jpn. J. Appl. Phys., **37** (1998) 3576.

[15] N. Nunoya et al.: The 11th Int. Conf. on Indium Phosphide and Related Materials (IPRM'99), Davos, TuB4-1, (1999).digest p. 349.

[16] M. Nakamura et al.: The 4th Optoelectronics and Commucations Conf. (OECC'99), Beijing, C65S, (1999).

[17] N. Nunoya et al.: The 1999 Int'l Conf. On Solid State Devices and Materials (SSDM'99), Tokyo, E-5-3, (1999).